

# **Improvements in FDS 6 and Development Update**

Kevin McGrattan

National Institute of Standards and Technology

Gaithersburg, Maryland, USA

Over the next few days, you will hear from:

Craig Weinschenk, NIST, Combustion

Kris Overholt, NIST, Automated Testing and V&V

Jason Floyd, Hughes-RJA, Baltimore, MD, Soot Deposition

Julio Goncalves da Silva, U. of Rio de Janeiro, Brazil, Fire-Structure Interface

Lukas Arnold, Juelich Supercomputing Centre, Germany, Parallel Processing

Susanne Kilian, hhpberlin, Germany, Pressure Solver

I will focus on:

Current validation efforts

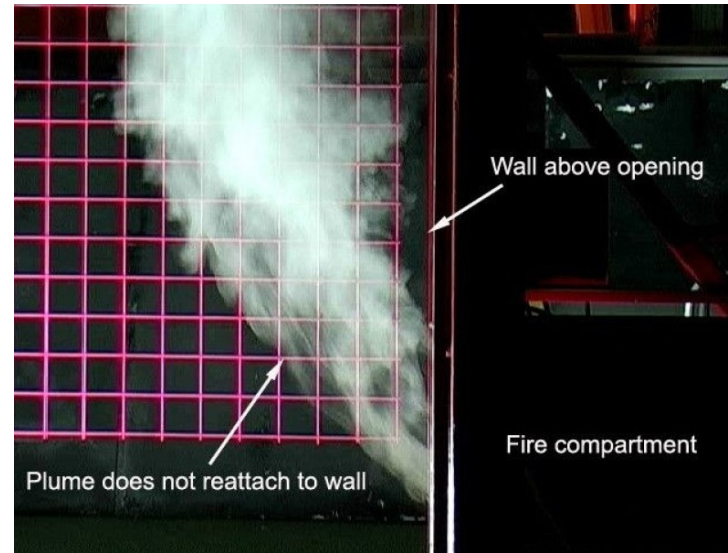
Pyrolysis

# Experimental Study of the Effects of Fuel Type, Fuel Distribution, and Vent Size on Full-Scale Underventilated Compartment Fires in an ISO 9705 Room

Andrew Lock  
Matthew Bundy  
Erik L. Johnsson  
Anthony Hamins  
Gwon Hyun Ko  
Cheolhong Hwang  
Paul Fuss  
Richard Harris



Smoke Venting Validation Experiments, Madrzykowski, Opert, Barowy



Spill Plumes, Harrison, Spearpoint, New Zealand

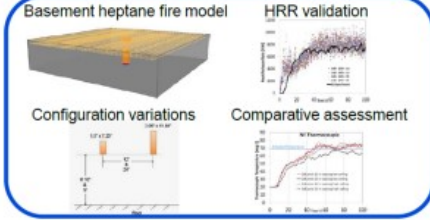


US Navy Hangar Experiments, Gott *et al.*

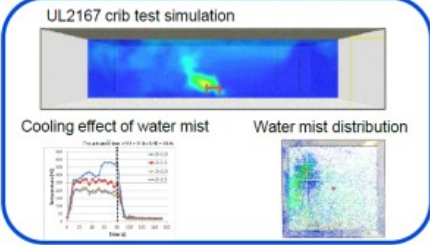
# Fire Suppression Modeling: Application

Proof of concept developed for applications of interest

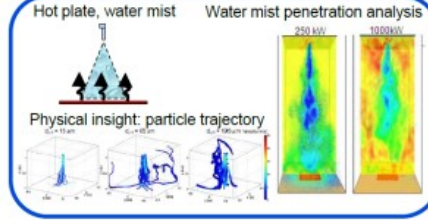
## Free burn: predict system activation time



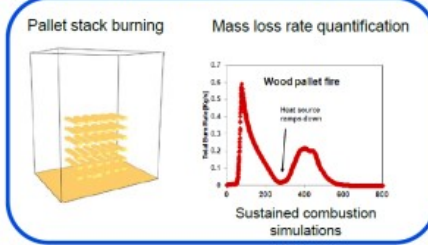
## Prescribed HRR: cooling, nozzles activation



## Buoyant plume: simulate water mist behavior

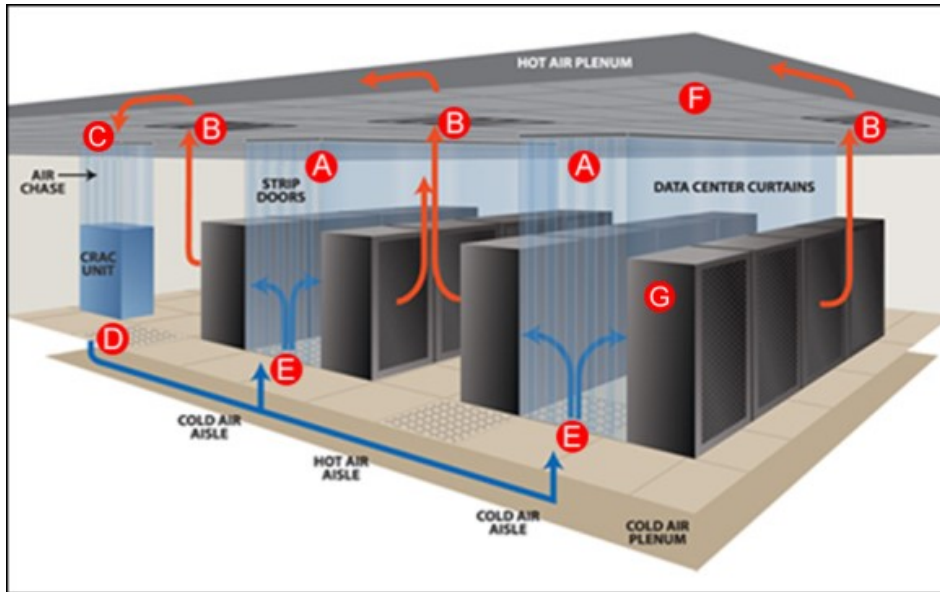


## Coupled: simulate suppression by water mist

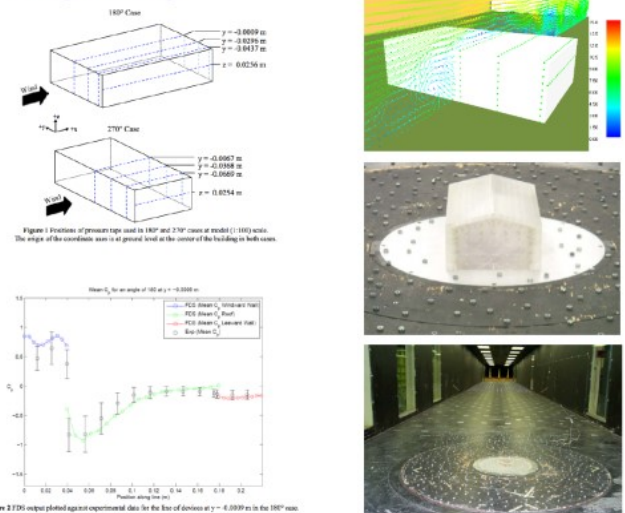


Any fuel package

Wood fire: crib, pallet



## Wind Engineering



Banerjee et al. (2012)

Ho et al. (2003)



## Heat and mass transfer due to a small-fire in an aircraft cargo compartment

Ezgi S. Oztekin\*

Technology and Management International, LLC (TMIL), 1403 Wainger Ave, Suite 300, Toms River, NJ 08710, United States

### ARTICLE INFO

Article history:  
Received 6 September 2013  
Received in final form 10 February 2014  
Accepted 10 February 2014  
Available online 14 March 2014

Keywords:  
Large eddy simulation  
Thermal plume engagement  
Near wall turbulence  
Buoyant heat flux  
Smoke transport  
Near-wall velocity

### ABSTRACT

The transport of smoke and hot gases induced by a prescribed fire-source in a confined enclosure is numerically studied. Large eddy simulations (LES) are performed using an open-source solver, the fire dynamics simulator (FDS) of the National Institute of Standards and Technology (NIST). For turbulence closure, the dynamic Smagorinsky and the constant-coefficient Vreman models, and for wall shear, the Werner and Wengle model are employed. Due to the small size of the fire-source, radiation is neglected in the calculations, however, its anticipated effects are discussed in the results. Furthermore, significance of near-wall treatments for heat flux, particularly, at the plume engagement region, is demonstrated. Requirements for near-wall resolution and effectiveness of wall heat flux functions are evaluated. The results are compared with the existing experimental data collected during the full-scale fire tests of the same set-up in which the enclosure was an empty aircraft cargo compartment entirely closed with no ventilation or leakage, and the fire-source was placed close to the middle of the compartment on the floor.

© 2014 Elsevier Ltd. All rights reserved.

### 1. Introduction

An inflight fire may have grave consequences if not detected before growing into an uncontrollable size. Fire detection is not critical, especially for the inaccessible areas of the aircraft, such as cargo compartments, where a direct visual inspection is not possible during flight. For aircraft fire safety, it is particularly critical to identify the fire at the very early stages when it is still small and its spread is limited. Understanding the fire dynamics, more specifically within our framework, the transport of induced smoke and hot gases as a result of a fire in an enclosure, is fundamental to the selection of successful detection methods. With this in mind, we investigate, numerically, the airflow induced by a prescribed fire-source in an empty aircraft cargo compartment with no ventilation and leakage. Although the specific area of interest is the inflight aircraft fire safety, the problem under consideration is, in fact, a canonical fire application, or even, because of the small fire-size, a natural convection problem, in which flow-field that is a transient heat-source in a confined enclosure is addressed.

There are two main mechanisms responsible for the scalar transport in an enclosure with a heat-source, namely, thermal plume and gravity current processes [1,2]. The thermal plume is

initiated by the buoyancy-induced upward gas movement; heated (low-density) gases ascend against the gravity-field, and are displaced with the entrained colder (heavier) ambient fluid. The mixing of the two expands the flow increasing the plume volume, decreasing the plume temperature and velocity away from the heat-source. The gravity currents are formed as a result of the impingement of the thermal plume on the ceiling leading to lateral spread of the second hot-gas along the enclosure walls. Depending on the momentum of the gravity current it either descends down the side walls or generate return flows increasing both stratification and mixing. As the plume continues to feed hot air into already formed gravity currents, the deepening of this hot-gas layer fills the enclosure from top to bottom. Since the temperature of the plume impinging on the ceiling is still higher than the temperature of the later-formed hot-gas layer, the plume maintains to create fluid, this time instead of the ambient fluid, from the hot-gas layer. Depending on the wall heat losses, temperature variation across the layer-height can be considerable.

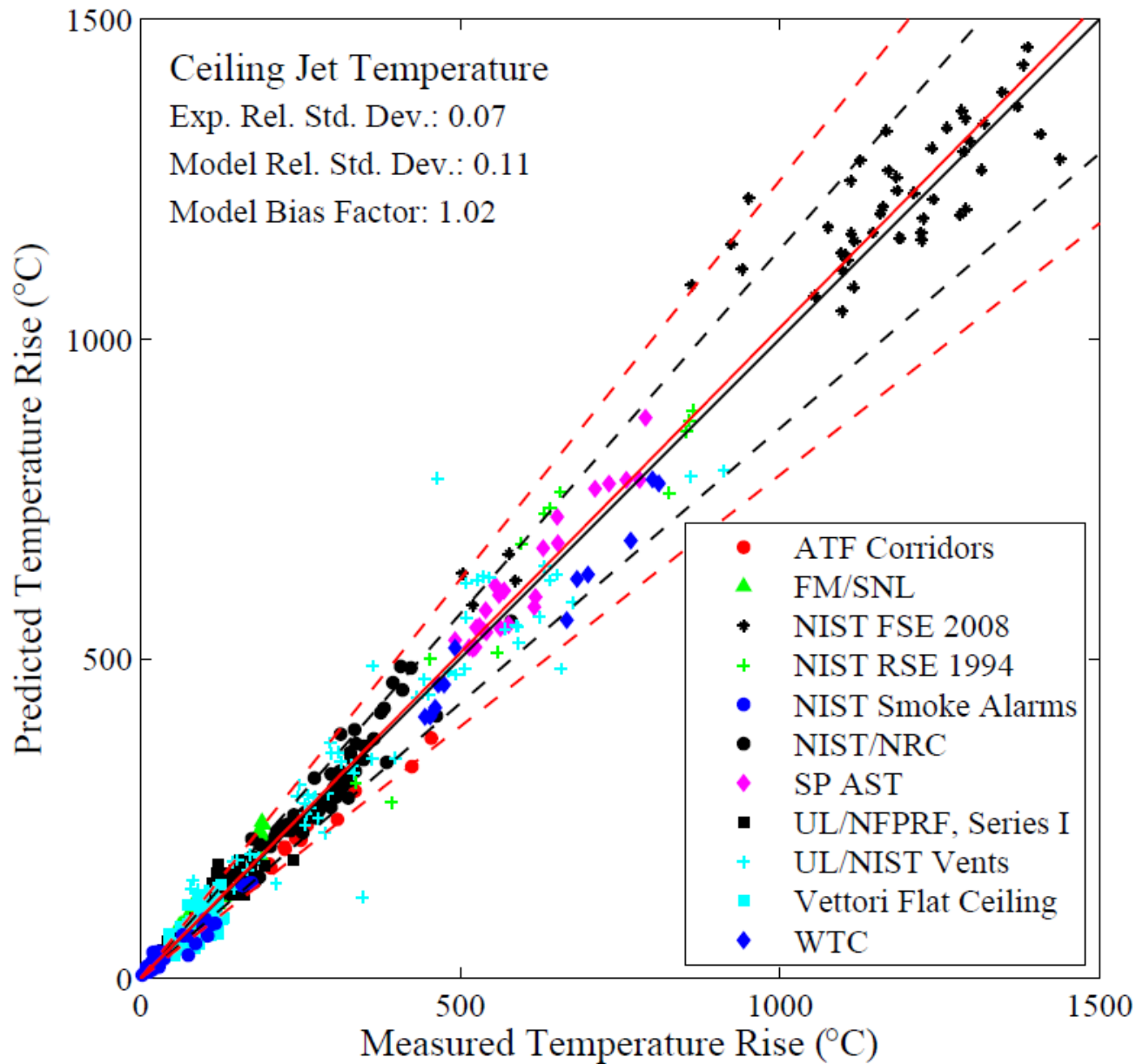
The convective heat-loss to the wall is critical in the overall flow behavior of thermal currents. It was demonstrated first with the experimental and later with the theoretical investigations that the corner-thickness and the spread-rate are affected substantially by heat losses [1,3]. Heat transfer for thermal currents were found to be much higher than that estimated for wall fire. This was explained by the existence of two-dimensional longitudinal

\* Tel.: +1 609 485 8363.

E-mail address: oztekin@tmil.com

http://dx.doi.org/10.1016/j.ijhmt.2014.02.019

0017-9310/2014 Elsevier Ltd. All rights reserved.



From *FDS Validation Guide*, Ceiling Jet chapter

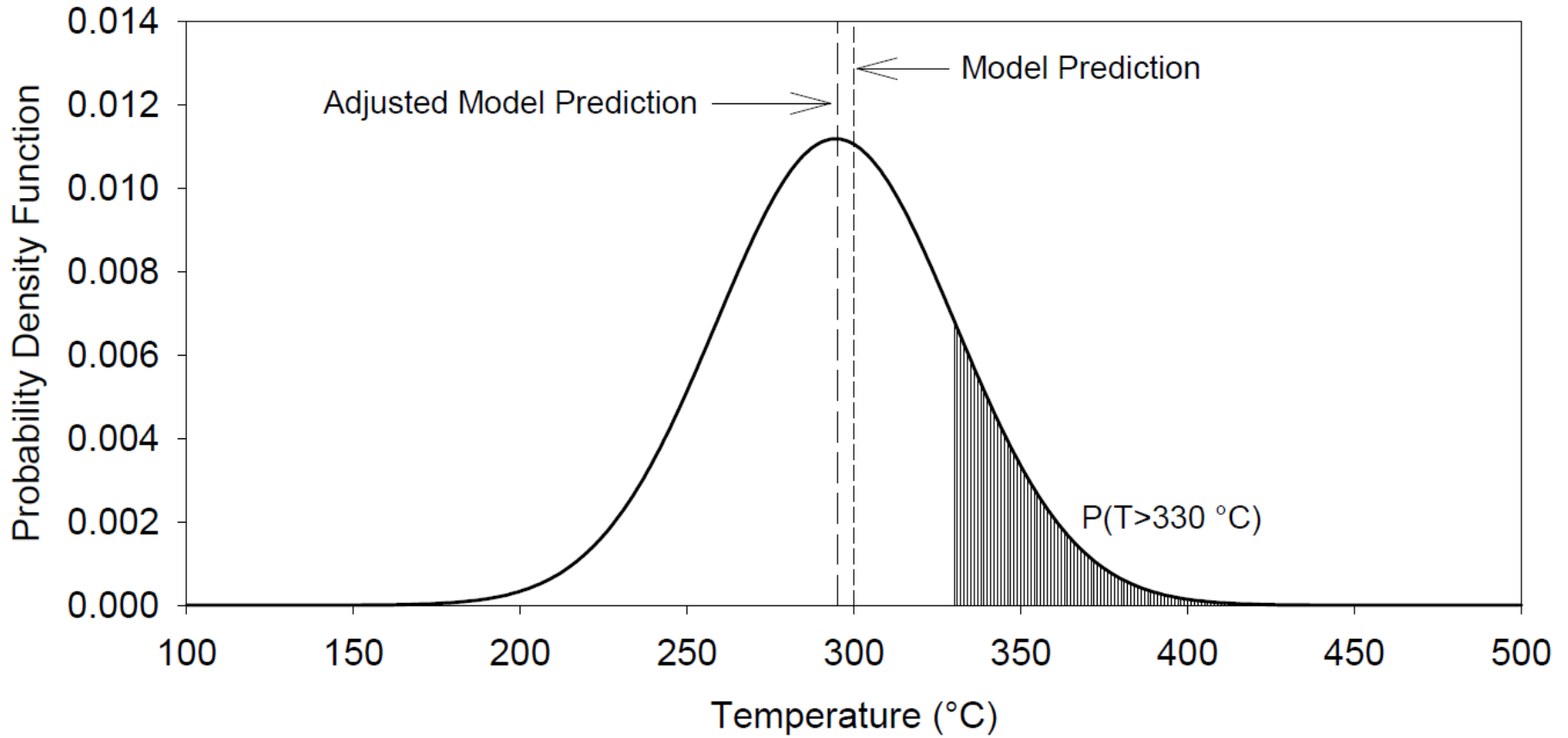


Table 15.1: Summary statistics for all quantities of interest

Quantity	Section	Datasets	Points	$\tilde{\sigma}_E$	$\tilde{\sigma}_M$	Bias
HGL Temperature, Forced Ventilation	5.12	4	111	0.07	0.22	1.27
HGL Temperature, Natural Ventilation	5.12	9	160	0.07	0.07	1.03
HGL Temperature, No Ventilation	5.12	3	32	0.07	0.13	1.23
HGL Depth	5.12	9	177	0.05	0.05	1.03
Ceiling Jet Temperature	7.1.13	11	552	0.07	0.11	1.02
Sloped Ceiling Jet Temperature	7.1.13	2	152	0.07	0.20	0.93
Plume Temperature	6.1.6	7	71	0.07	0.19	1.13
Oxygen Concentration	9.1.4	5	98	0.08	0.11	0.99
Carbon Dioxide Concentration	9.1.4	6	95	0.08	0.11	0.98
Smoke Concentration	9.2.1	1	14	0.19	0.60	2.63
Compartment Over-Pressure	10.3	2	39	0.21	0.23	0.98
Open Compartment Over-Pressure	10.3	2	14	0.15	0.27	1.02
Target Temperature	11.2.4	4	819	0.07	0.21	1.00
THIEF Temperature	11.3.3	2	94	0.07	0.16	1.06
Surface Temperature	11.1.5	3	845	0.07	0.13	1.04
Target Heat Flux	12.2.5	3	267	0.11	0.27	0.98
Flame Impinging Heat Flux	12.1.8	4	52	0.11	0.36	0.93
Surface Heat Flux	12.1.8	2	342	0.11	0.16	0.91
Velocity	8.7	6	211	0.08	0.09	1.00
Sprinkler Activation Time	7.2.1	5	232	0.06	0.15	0.93
Smoke Detector Activation Time	7.3	1	142	0.26	0.26	0.62
Smoke Detector Activation Time, Temp. Rise	7.3	1	142	0.29	0.29	0.86
Cable Failure Time	11.3.4	1	35	0.12	0.16	1.10
Sprinkler Actuations	7.2.2	3	38	0.15	0.29	0.96
Burning Rate	14.5	2	30	0.08	0.21	1.08
Carbon Monoxide Concentration	9.3.5	5	69	0.19	0.41	0.91
Entrainment	6.3	2	87	0.05	0.05	1.12
Extinction Time	13.2	1	39	0.10	0.62	1.96
Species Concentration	9.4	1	126	0.08	0.15	0.98
Low Ceiling Jet Temperature	7.1.13	1	120	0.07	0.15	1.12
Low Heat Flux	12.1.8	2	18	0.11	0.44	0.97
Low Surface Temperature	11.1.5	1	6	0.07	0.28	1.04
Smoke Obscuration	9.2.2	1	18	0.18	0.18	1.01

Table 3.10: Summary of important experimental parameters.

Test Series	$\dot{Q}$ (kW)	$D$ (m)	$H$ (m)	$\dot{Q}^*$	$L_f/H$	$\phi$	$W/H$	$L/H$	$r_{cj}/H$	$r_{rad}/D$
Arup Tunnel	5344	1.6	7	1.5	0.8	0.0	1.1	43	0.0 – 1.1	N/A
ATF Corridors	50 – 500	0.5	2.4	0.3 – 3.3	0.3 – 0.9	0.0 – 0.1	0.8	7.1	0.8 – 6.0	N/A
Beyler Hood	8 – 30	0.2	0.5	0.5 – 1.1	0.7 – 1.3	0.2 – 1.7	2.0	2.0	N/A	N/A
Bryant Doorway	34 – 511	0.3	2.4	0.5 – 6.9	0.2 – 1.0	0.0 – 0.2	1.0	2.1	0.6 – 0.8	N/A
Cup Burner	0.3	0.028	Open	2.1	Open	Varying	Open	Open	Open	N/A
FAA Cargo	5	0.1	1.4	1.4	0.2	0.2	2.3	4.8	0.1 – 4.8	N/A
Fleury Heat Flux	100 – 300	0.3 – 0.6	Open	0.3 – 5.5	Open	Open	Open	Open	Open	1.7 – 3.3
FM Panels	30 – 100	0.5	Open	0.2 – 0.5	Open	Open	Open	Open	Open	0
FM/SNL	470 – 516	0.9	6.1	0.6 – 2.4	0.3 – 0.6	0.0 – 0.2	2.0	3.0	0.2 – 0.3	N/A
Hamins CH <sub>4</sub>	0.4 – 162	0.1 – 1.0	Open	0.1	Open	Open	Open	Open	N/A	0.1 – 12
Harrison Plumes	5 – 15	0.16	0.5	0.5 – 1.4	0.5 – 1.0	Open	Open	Open	N/A	N/A
Heskestad	10 <sup>2</sup> – 10 <sup>7</sup>	1.1	Open	10 <sup>-1</sup> – 10 <sup>4</sup>	Open	Open	Open	Open	N/A	N/A
LLNL Enclosure	50 – 400	0.6	4.5	0.2 – 1.5	0.1 – 0.4	0.1 – 0.4	0.9	1.3	0.3 – 1.0	N/A
McCaffrey Plume	14 – 57	0.3	Open	0.2 – 0.8	Open	Open	Open	Open	N/A	N/A
NBS Multi-Room	110	0.3	2.4	1.5	0.5	0.0	1.0	5.1	N/A	N/A
NIST FSE	100 – 2500	0.6 – 1.1	2.4	0.5 – 1.8	0.4 – 1.7	0.2 – 5.9	1.0	1.5	0.4 – 0.8	N/A
NIST/NRC	350 – 2200	1.0	3.8	0.3 – 2.0	0.3 – 1.0	0.0 – 0.3	1.9	5.7	0.3 – 2.1	2.0 – 4.0
NIST RSE	50 – 600	0.15	1.0	5.2 – 63	0.9 – 2.8	0.1 – 1.1	1.0	1.5	N/A	N/A
NIST Smoke Alarms	100 – 350	1.0	2.4	0.2 – 0.3	0.2 – 0.5	N/A	1.7	8.3	1.3 – 8.3	N/A
NRCC Facade	5000 – 10300	4.3	2.8	0.1 – 0.2	0.9 – 1.7	0.6 – 1.2	1.6	2.2	N/A	0
NRL/HAI	50 – 520	0.3 – 0.7	Open	1.1 – 1.2	Open	Open	Open	Open	N/A	0
Sandia Plume	2025 – 5450	1.0	Open	1.8 – 5.0	Open	Open	Open	Open	N/A	N/A
SP AST	450	0.3	2.4	6.1	1.1	0.1	1.0	1.5	N/A	N/A
Steckler	31.6 – 158	0.3	2.1	0.8 – 3.8	0.3 – 0.7	0.0 – 0.6	1.3	1.3	N/A	N/A
UL/NFPRF	4400 – 10000	1.0	7.6	4.0 – 9.1	0.7 – 1.0	Open	4.9	4.9	0.6 – 3.9	N/A
UL/NIST Vents	500 – 2000	0.9	2.4	0.7 – 2.6	0.8 – 1.6	0.2 – 0.6	1.8	2.5	1.0 – 2.3	N/A
Ulster SBI	30 – 60	0.2	Open	1.5 – 3.0	Open	Open	Open	Open	N/A	0
USCG/HAI	250 – 1000	0.3	3.0	6.0 – 24	0.6 – 1.1	0.3 – 1.0	1.7	2.3	N/A	N/A
USN Hawaii	100 – 7700	0.3 – 2.5	15	0.7 – 1.3	0.1 – 0.4	Open	4.9	6.5	0 – 1.2	N/A
USN Iceland	100 – 15700	0.3 – 3.4	22	0.7 – 1.3	0.0 – 0.3	Open	2.1	3.4	0 – 1.0	N/A
Vettori Flat	1055	0.7	2.6	2.5	1.1	0.3	2.1	3.5	0.8 – 2.9	N/A
Vettori Sloped	1055	0.7	2.5	2.5	1.2	0.3	2.2	2.9	N/A	N/A
VTT Large Hall	1860 – 3640	1.4 – 1.8	19	0.7	0.2	0	1.0	1.4	0 – 0.6	N/A
WTC	1970 – 3240	1.6	3.8	0.6 – 0.9	0.8 – 1.1	0.3 – 0.5	0.9	1.8	0.0 – 0.8	0.3 – 1.3



# Verification and Validation of Selected Fire Models for Nuclear Power Plant Applications

## Supplement 1

Draft Report for Comment

U.S. Nuclear Regulatory Commission  
Office of Nuclear Regulatory Research  
Washington, DC 20555-0001

Electric Power Research Institute  
3420 Hillview Avenue  
Palo Alto, CA 94304



# Verification and Validation of FDS, CFAST, Empirical Correlations, recently updated for US NRC

Table 5-1. Summary of model uncertainty metrics.

Output Quantity	Empirical Correlations			CFAST		MAGIC		FDS		Exp
	Corr.	$\delta$	$\tilde{\sigma}_M$	$\delta$	$\tilde{\sigma}_M$	$\delta$	$\tilde{\sigma}_M$	$\delta$	$\tilde{\sigma}_M$	$\tilde{\sigma}_E$
HGL Temp. Rise, Natural	MQH	1.17	0.15	1.20	0.34	1.13	0.30	1.00	0.12	0.07
HGL Temp. Rise, Forced	FPA	1.29	0.32	1.15	0.20	1.08	0.17	1.21	0.22	0.07
	DB	1.18	0.25							
HGL Temp. Rise, Closed	Beyler	1.04	0.37	0.99	0.08	1.07	0.16	1.20	0.12	0.07
HGL Depth	ASET/YT	-	-	1.12	0.36	1.17	0.31	1.03	0.06	0.05
Ceiling Jet Temp. Rise	Alpert	0.86	0.11	1.18	0.33	1.04	0.45	0.98	0.14	0.07
Plume Temp. Rise	Heskestad	0.84	0.33	1.08	0.20	1.04	0.20	1.20	0.21	0.07
	McCaffrey	0.90	0.31							
Oxygen Concentration	N/A			1.00	0.15	0.93	0.22	1.01	0.11	0.08
Smoke Concentration	N/A			3.16	0.68	3.71	0.66	2.63	0.59	0.19
Pressure Rise	N/A			1.36	0.66	1.49	0.45	0.96	0.27	0.21
Target Temp. Rise	Steel	1.29	0.45	1.58	0.64	1.08	0.38	0.98	0.18	0.07
Target Heat Flux	Point Source	1.44	0.47	0.93	1.16	0.85	0.66	0.98	0.25	0.11
	Solid Flame	1.17	0.44							
Surface Temp. Rise	N/A			1.05	0.28	0.95	0.29	0.99	0.12	0.07
Surface Heat Flux	N/A			0.98	0.34	0.78	0.35	0.92	0.15	0.11
Cable Failure Time	THIEF	0.90	0.11	-	-	-	-	1.10	0.16	0.12
Sprinkler Activation Time	Sprinkler	1.11	0.41	0.80	0.21	0.91	0.20	0.93	0.15	0.06
Smoke Detector Act. Time	Temp. Rise	0.66	0.57	1.12	0.46	1.54	0.36	0.85	0.29	0.34

# A Brief History of Pyrolysis and Flame Spread Modeling in FDS

# Flame Spread in Microgravity, 1990-2000

T. Kashiwagi, H. Baum, K. McGrattan, W. Mell, S. Olson (NASA)



$$\text{Mass } \frac{\partial(\rho_S/\rho_{S0})}{\partial t} = -(1 - \nu_{C,p})\dot{\omega}_p$$

$$- (1 - \nu_{C,ox})\dot{\omega}_{ox}$$

$$- (1 - \nu_{A,char})\dot{\omega}_{char}$$

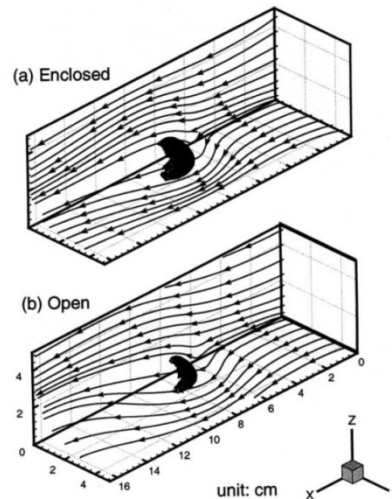
$$\text{Pyrolysis: } \dot{\omega}_p = B_p \left( \frac{\rho_S}{\rho_{S0}} Y_F \right)^{n_{F,p}} \exp \left( - \frac{E_p}{RT_S} \right)$$

Pyrolysis reaction parameter [10, 16]

$B_p$ : frequency factor; 1/s	$3.0 \times 10^{18}$
$E_p$ : activation energy; kJ/mole	237
$n_{F,p}$ : exponent of $Y_F$	1.2
$\nu_{C,p}$ : mass-based stoich. constant	0.14
$\nu_{f,p}$ : mass-based stoich. constant	0.23
$q_p$ : heat of combustion; J/g	64

Thermal- & physical properties [10]

$c_{pS}$ : specific heat of solid; J/(gK)	$0.96 + 4.19 \times (T-300)$
$k_S$ : thermal conductivity of solid; W/(cmK)	$3.55 + 1.55 \times 10^{-2} \times (T-300)$
$\delta$ : thickness of solid; cm	0.013
$\rho_S$ : surface density; g/cm <sup>2</sup>	$5.7 \times 10^{-3}$
$\epsilon$ : surface emissivity	0.6
$r$ : surface reflectivity	0.25



## Enclosure Effects on Flame Spread Over Solid Fuels in Microgravity<sup>‡</sup>

YUJI NAKAMURA,<sup>†,\*</sup> TAKASHI KASHIWAGI, KEVIN B. MCGRATTAN, and HOWARD R. BAUM

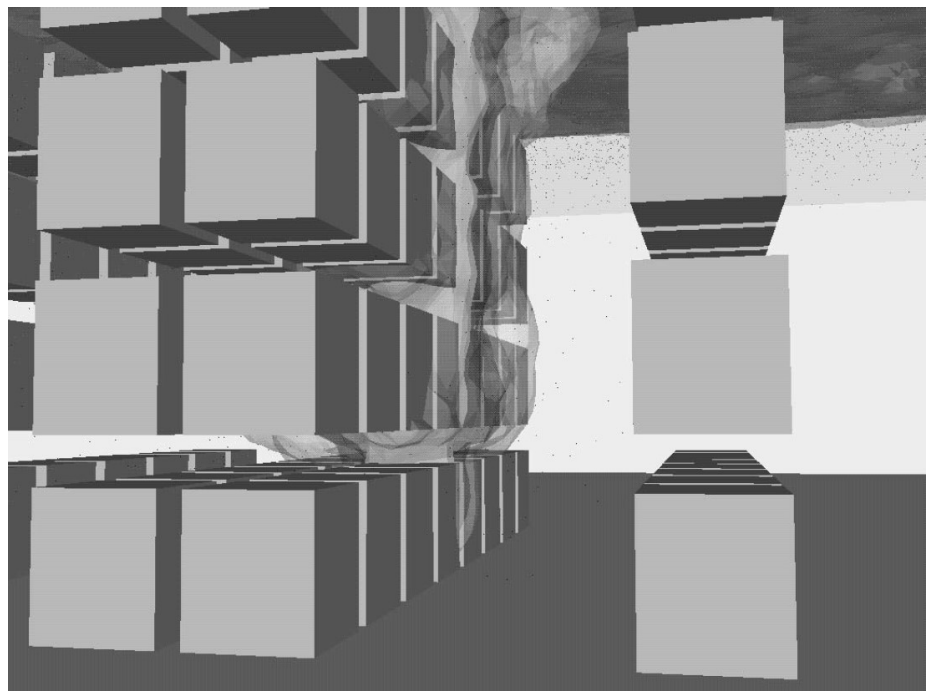
Building and Fire Research Laboratory, National Institute of Standard and Technology, 100 Bureau Dr., Mail Stop 8663, Gaithersburg, MD 20899-8663 USA

Microgravity flame spread experiments, S. Olson, NASA

Fire Research Foundation  
Sprinkler, Vent, Draft Curtain Study  
1995-1998



Small scale suppression experiments, A. Hamins (NIST), D. Sheppard (UL)

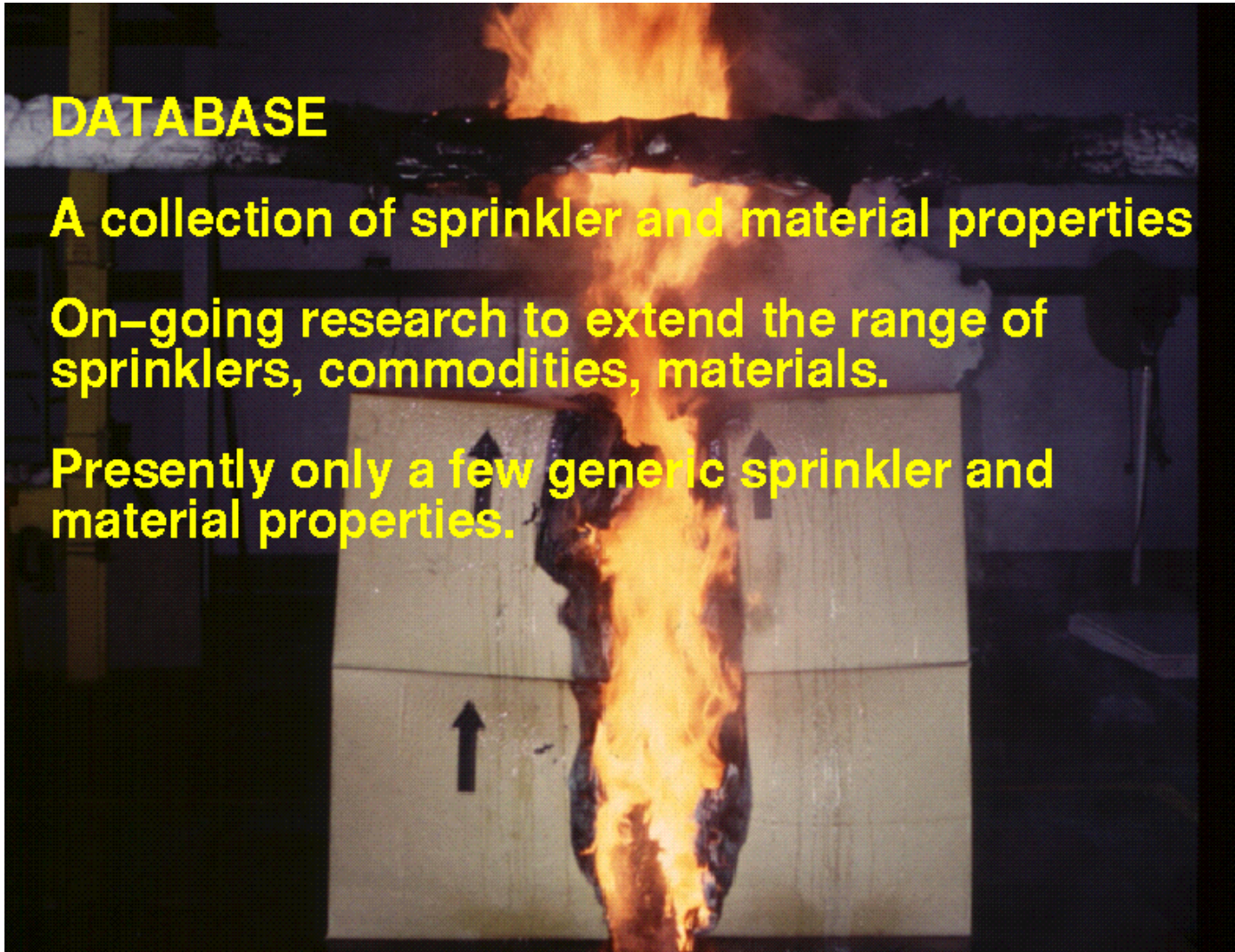


## **DATABASE**

**A collection of sprinkler and material properties**

**On-going research to extend the range of sprinklers, commodities, materials.**

**Presently only a few generic sprinkler and material properties.**

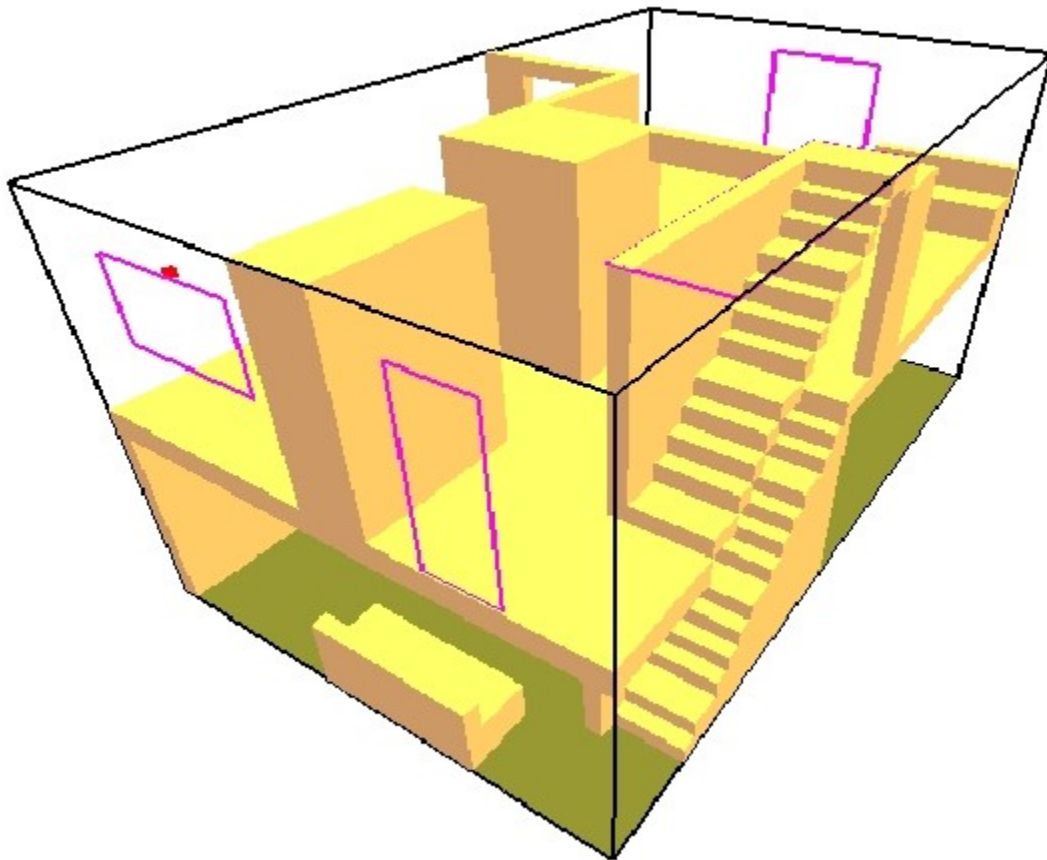


A slide from a presentation at the 2000 Fire Research Foundation Suppression and Detection Meeting, Orlando, Florida

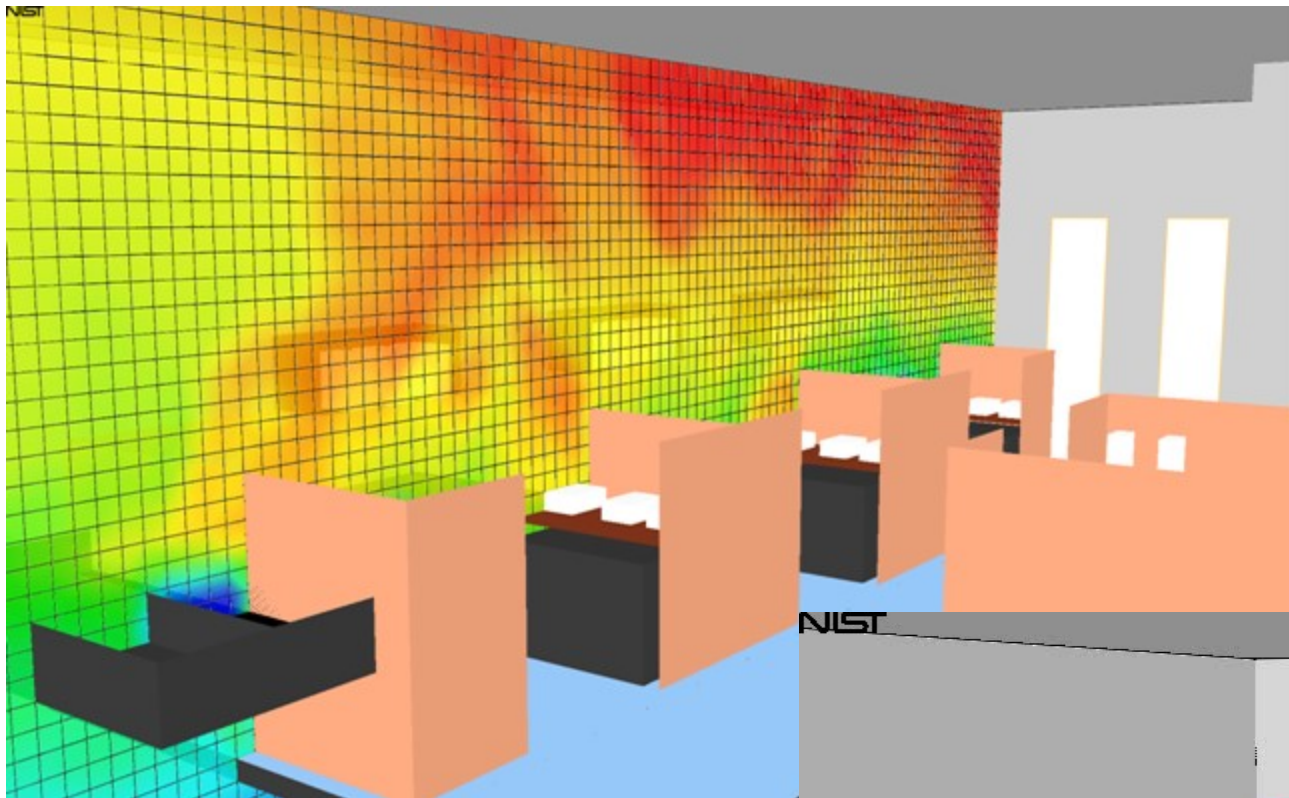
# Investigation of a Fatal House Fire Washington, DC, 2000

D. Madrzykowski and R. Vettori

NIST Smokeview 1.0.1A

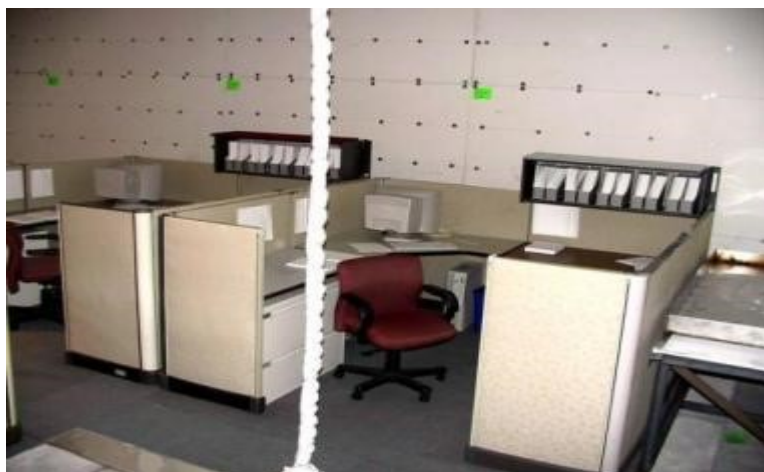


NIST



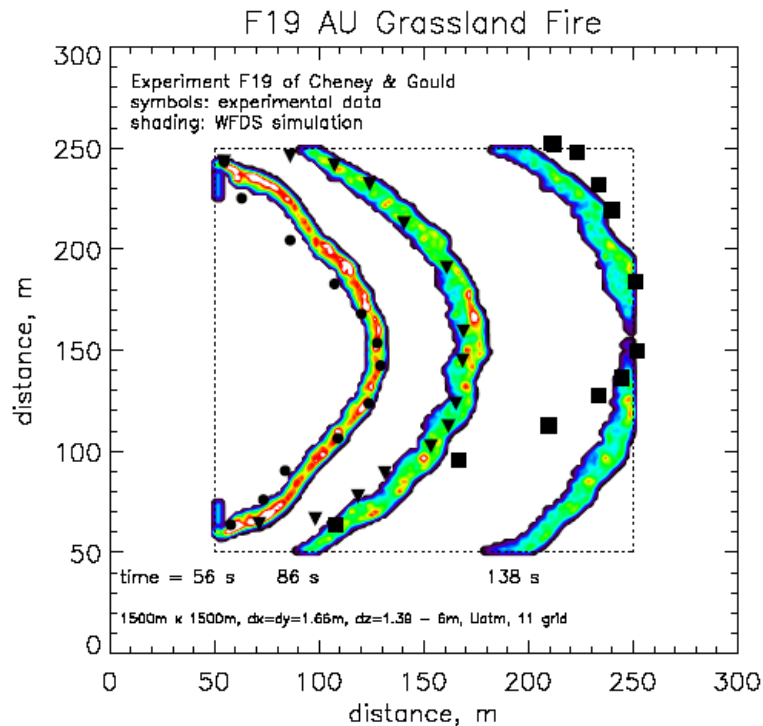
# WTC Investigation 2001-2005

NIST



# Simulations of Australian Grassland Fires

## Ruddy Mell (NIST, Forest Service), 2000-Present



- Head fire spread rate well predicted.
- Need more testing of flank fire prediction.



- height = 51 cm
- loading =  $0.31 \text{ kg m}^{-2}$
- moisture = 4.8%
- $U_2 = 4.8 \text{ ms}^{-1}$
- surface/volume =  $12200 \text{ m}^{-1}$
- $L_{ig} = 175 \text{ m}$



Cable Fire Experiments and Modeling on behalf of US and Finnish Nuclear Regulatory Authorities, 2007-Present



Cable Fire Experiments, K. McGrattan, NIST

SCIENCE • TECHNOLOGY RESEARCH HIGHLIGHTS • SECTIONS

Dissertation  
44

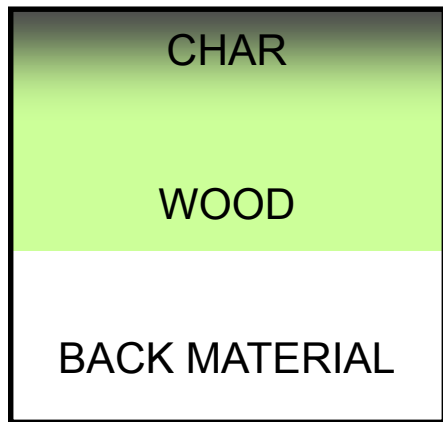
**Methods and applications  
of pyrolysis modelling for  
polymeric materials**

Anna Matala

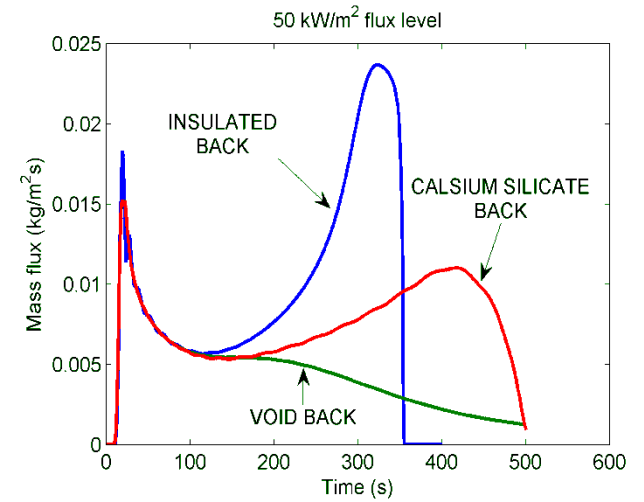
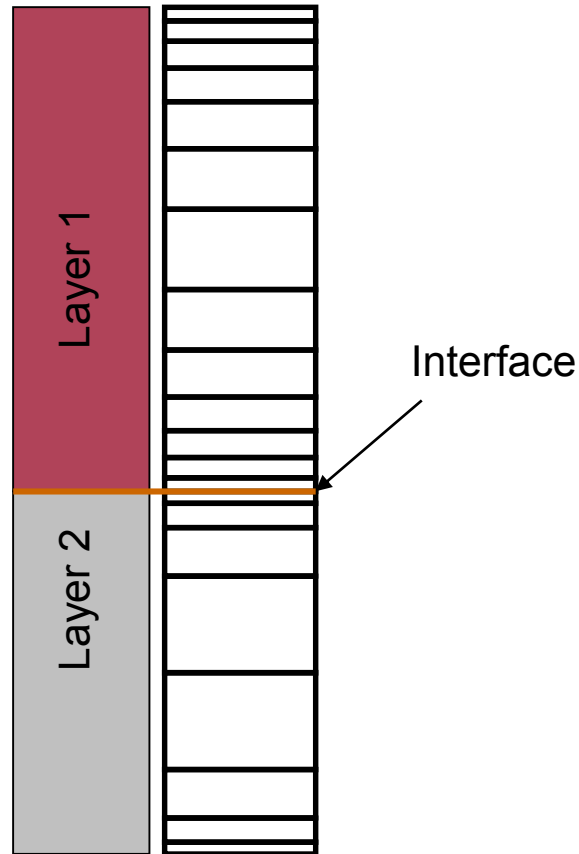
VTT

# Pyrolysis Model in FDS

S. Hostikka, VTT, Finland, 2003



BACK SIDE BC



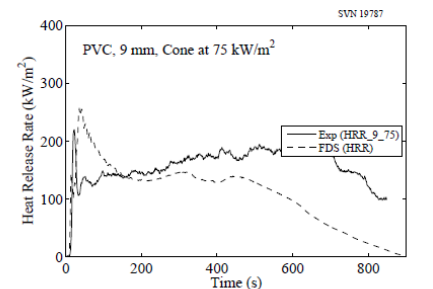
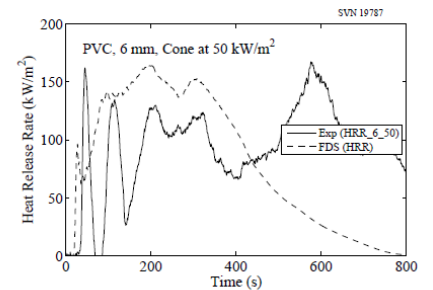
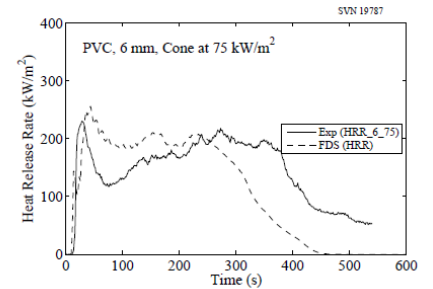
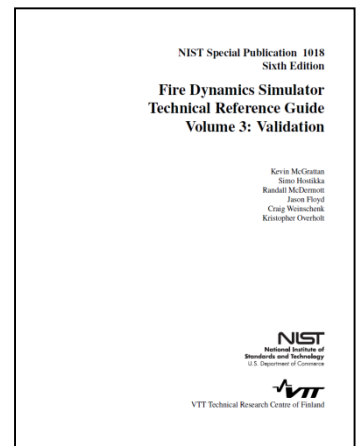
# Charring and Non-Charring Polymers

S. Stoliarov (Maryland), K. McGrattan (NIST)



Table 14.4: Properties of poly(vinyl chloride) (PVC). Courtesy S. Stoliarov, University of Maryland. See Section 14.1.1 for an explanation of terms.

Property	Units	Value	Method	Reference
Polymer Density	kg/m <sup>3</sup>	1430 ± 70	Direct	[141]
Polymer Conductivity	W/m/K	0.17 ± 0.01	Literature	[141]
Polymer Specific Heat	kJ/kg/K	1.55 ± 0.25	DSC	[216]
Polymer Emissivity		0.90 ± 0.05	IS	[217]
Polymer Absorption Coef.	m <sup>-1</sup>	2145 ± 715	FTIR	[218]
Char 1 Density	kg/m <sup>3</sup>	629	Constant Volume	[141]
Char 1 Conductivity	W/m/K	0.17	Inherited	[141]
Char 1 Specific Heat	kJ/kg/K	1.55 ± 0.25	Inherited	[141]
Char 1 Emissivity		0.90 ± 0.05	Inherited	[141]
Char 1 Absorption Coef.	m <sup>-1</sup>	2453	Inverse Analysis	[141]
Char 2 Density	kg/m <sup>3</sup>	296	Constant Volume	[141]
Char 2 Conductivity	W/m/K	0.26	Inverse Analysis	[141]
Char 2 Specific Heat	kJ/kg/K	1.72 ± 0.17	Pulsed Current	[141, 220]
Char 2 Emissivity		0.85 ± 0.05	Pulsed Current	[141, 220]
Char 2 Absorption Coef.	m <sup>-1</sup>	Opaque	Assumption	[141]
Reac 1 Pre-Exp. Factor	s <sup>-1</sup>	$(1.4 \pm 0.8) \times 10^{33}$	TGA	[141]
Reac 1 Activation Energy	kJ/kmol	$(3.67 \pm 0.07) \times 10^5$	TGA	[141]
Reac 1 Char Yield		0.44 ± 0.01	TGA	[141]
Reac 1 Heat of Reaction	kJ/kg	170 ± 17	DSC	[216]
Gas 1 Heat of Combustion	kJ/kg	2700 ± 300	MCC	[141]
Gas 1 Combustion Efficiency		0.75 ± 0.03	Cone Calorimeter	[141]
Reac 2 Pre-Exp. Factor	s <sup>-1</sup>	$(3.5 \pm 2.1) \times 10^{12}$	TGA	[141]
Reac 2 Activation Energy	kJ/kmol	$(2.07 \pm 0.04) \times 10^5$	TGA	[141]
Reac 2 Char Yield		0.47 ± 0.01	TGA	[141]
Reac 2 Heat of Reaction	kJ/kg	1200 ± 900	DSC	[216]
Gas 2 Heat of Combustion	kJ/kg	36500 ± 1800	MCC	[141]
Gas 2 Combustion Efficiency		0.75 ± 0.03	Cone Calorimeter	[141]



## Flame/Fire Spread Modeling – What is the problem?

1. Each application is special and requires a multi-year effort.
2. Usually full-scale experiments are required to calibrate model parameters.
3. It is difficult to reproduce results with different codes or code versions.
4. There is no generally accepted methodology for measuring input parameters.
5. The driving force for flame spread modeling is forensic investigation rather than performance-based design.